THE JOURNAL OF
PHYSICAL CHEMISTRY A

Article

pubs.acs.org/JPCA

Kinetics and Mechanisms of the Thermal Decomposition of 2-Methyl-1,3-dioxolane, 2,2-Dimethyl-1,3-dioxolane, and Cyclopentanone Ethylene Ketal in the Gas Phase. Combined Experimental and DFT Study

Felix Rosas,[†] Jesus Lezama,[†] José R. Mora,[†] Alexis Maldonado,[†] Tania Cordova,[‡] and Gabriel Chuchani*,[†]

[†]Centro de Química, Instituto Venezolano de Investigaciones Científicas (I.V.I.C.), Apartado 21827, Caracas 1020.A, Venezuela
[‡]Department of Medicinal Chemistry, College of Pharmacy, University of Florida, P.O. Box 100485, Gainesville, Florida 32610, United States

S *Supporting Information*

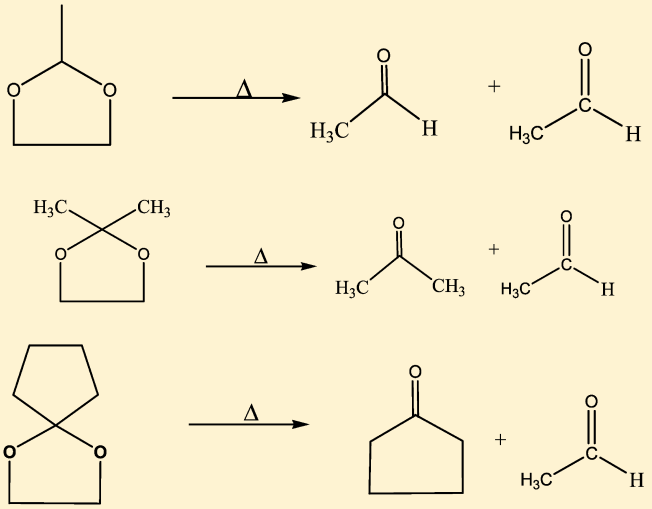

ABSTRACT: The kinetics of the gas-phase thermal decomposition of 2-methyl-1,3-dioxolane, 2,2-dimethyl-1,3-dioxolane, and cyclopentanone ethylene ketal were determined in a static system and the reaction vessel deactivated with allyl bromide. The decomposition reactions, in the presence of the free radical suppressor propene, are homogeneous, are unimolecular, and follow first-order law kinetics. The products of these reactions are acetaldehyde and the corresponding ketone. The working temperature range was 459−490 °C, and the pressure range was 46−113 Torr. The rate coefficients are given by the following Arrhenius equations: for 2-methyl-1,3-dioxolane, $\log k = (13.61 \pm 0.12) - (242.1 \pm 1.0)(2.303RT)^{-1}$, $r = 0.9997$; for 2,2-dimethyl-1,3-dioxolane, $\log k = (14.16 \pm 0.14) - (253.7 \pm 2.0)(2.303RT)^{-1}$, $r = 0.9998$; for cyclopentanone ethylene ketal, $\log k = (14.16 \pm 0.14) - (253.7 \pm 2.0)(2.303RT)^{-1}$, $r = 0.9998$. Electronic structure calculations using DFT methods B3LYP and MPW1PW91 with 6-31G(d,p), and 6-31++G(d,p) basis sets suggest that the decomposition of these substrates takes place through a stepwise mechanism. The rate-determining step proceeds through a concerted nonsynchronous four-centered cyclic transition state, and the elongation of the C−OCH_3 bond in the direction $C_\alpha^{\delta+}\ldots OCH_3^{\delta-}$ is predominant. The intermediate products of these decompositions are unstable, at the working temperatures, decomposing rapidly through a concerted cyclic six-centered cyclic transition state type of mechanism.

I. INTRODUCTION

Several investigations of Molera et al.[1−6] on the thermal decomposition of ketals led to the idea that the C−OR bond polarization may be rate-determining (Scheme 1). In addition, the presence of a C_β−H bond was believed to be important in the transition state mechanism from the work on the decomposition kinetics of 2,2-diethoxy ethylamine and 2,2-diethoxy-*N*,*N*-diethyl ethylamine in the gas phase.[7]

Scheme 1

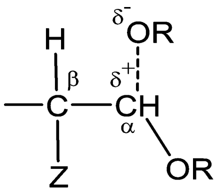

Z = Substituent
R = Alkyl

The previous works led to the examination of the homogeneous, unimolecular, gas-phase decomposition kinetics of several β-substituted diethyl acetals (reaction 1).[8] The reactions were thought to proceed via two parallel reactions as described in reaction 1. The kinetic and thermodynamic parameters of the parallel reactions suggested two different concerted polar four-membered cyclic transition state mechanisms.

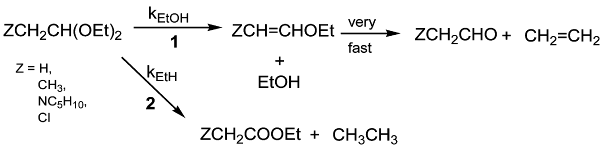

(1)

Received: May 28, 2012
Revised: August 9, 2012
Published: August 10, 2012

Scheme 2[a]

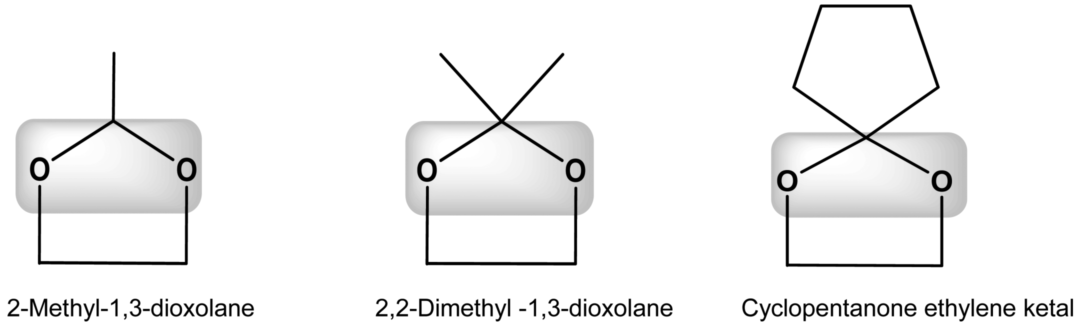

[a]The ketal functional group is depicted in grey shadow.

Further studies on ketals had been reported; for example, the thermal decomposition kinetics of 1,1-dimethoxycyclohexane yielded 1-methoxycyclohexene and methanol.[9] Theoretical calculations about the elucidation of the mechanism of this reaction[9] were carried out using DFT methods. The estimated values for the energy and enthalpy of activation showed reasonably good agreement with the experimental values with a PBEPBE/6-31G (d,p) level of theory. Experimental and theoretical results suggested a concerted polar four-membered cyclic transition state type of mechanism.

Recently, a joint experimental and theoretical study on the decomposition kinetics of ketals, but without an α−H at the carbon containing the two alkoxy groups, 2,2-diethoxypropane and 1,1-diethoxycyclohexane,[10] was carried out. The results of this work demonstrated that these reactions take place through a concerted nonsynchronous four-centered cyclic transition state type of mechanism as described in reactions 2 and 3. The predicted rate-determining step is the polarization of the C−O bond. The intermediate product of the 2,2-diethoxypropane decomposition, 2-ethoxypropene, further decomposes through a concerted cyclic six-centered cyclic transition state mechanism, as reported for gas-phase decomposition of alkyl vinyl ethers[11,12] (reaction 2, step 2) to a carbonyl compound.

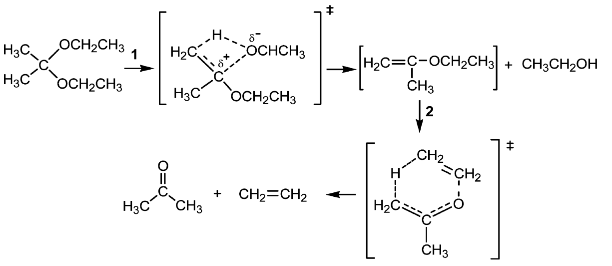

(2)

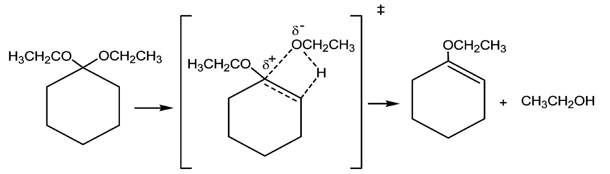

(3)

In association with the ketal functional group, it seemed interesting to investigate the thermal decomposition kinetics when both oxygen atoms attached to a carbon atom are members of a heterocyclic structure. In addition to this fact, the presence of a hydrogen atom of the adjacent C−H bond to the $-C(O)_2-$ is required in the assistance of the decomposition process and must be outside of the heterocyclic geometry. In this respect, the substrates to be examined are 2-methyl-1,3-dioxolane, 2,2-dimethyl-1,3-dioxolane, and cyclopentanone ethylene ketal (Scheme 2). For reasonable mechanistic interpretations, theoretical calculations were carried out along the minimum energy path, in order to obtain the kinetic parameters as a means to understand the nature of the molecular processes of these reactions.

II. EXPERIMENTAL SECTION

The starting materials 2-methyl-1,3-dioxolane, 2,2-dimethyl-1,3-dioxolane, and cyclopentanone ethylene ketal were acquired from Aldrich and used after distillation to better than 98.5% purity. Analyses of these substrates were conducted using a GC/MS Saturn 2000, Varian instrument with a DB-5MS capillary column of 30 m × 0.53 mm i.d. and 1.5 μm film thickness. The products were identified using a GC/MS Saturn 2000, Varian instrument with a DB-5MS capillary column of 30 m × 0.25 mm i.d. and 0.25 μm film thickness. For quantitative analysis of the products, a Varian 3700 gas chromatograph with Porapak S (80−100 mesh) 4 m and Chromosorb 103 (80−100 mesh) 4 m columns was used for acetone and cyclopentanone characterization, respectively.

Kinetics. The kinetic measurements were carried out in a static reaction system as previously described.[13−16] The wall of the reaction vessel was deactivated with the product of decomposition of allyl bromide at approximately 400 °C. In our experiments, several runs were performed at each temperature. The rate coefficients were calculated from a pressure increase measured manometrically and by the quantitative GC analysis. The temperature was controlled by a resistance thermometer controller, SHINKO DIC-PS 25RT, maintained within ±0.2 °C and measured with a calibrated 13% platinum−platinum rhodium thermocouple. No temperature gradient was found along the reaction vessel. The substrates were all injected directly into the reaction vessel with a syringe through a silicone rubber septum. The amount of reactant used for each kinetic run was ~0.05−0.2 mL.

III. RESULTS AND DISCUSSION

The products' formation in the molecular decomposition of 2-methyl-1,3-dioxolane, 2,2-dimethyl-1,3-dioxolane, and cyclopentanone ethylene ketal, in vessels deactivated with allyl bromide, are described in reactions 4−6.

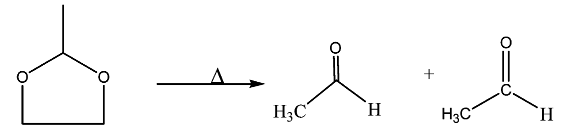
(4)

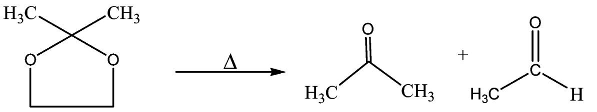
(5)

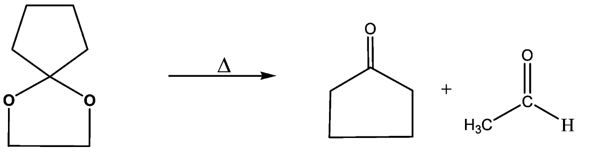
(6)

The homogeneity of these reactions was examined by carrying out several runs in a vessel with a surface-to-volume ratio of 6.0, relative to that of the normal vessel which is equal to 1.0 (Table 1). The packed and unpacked Pyrex vessel, seasoned with allyl bromide, had no effect on rates. However, the packed and unpacked clean Pyrex vessel resulted in a very significant heterogeneous effect in the rate coefficients.

Table 1. Homogeneity of the Reaction

substrate	T (°C)	S/V (cm^{-1})[a]	$10^4 k_1$ s^{-1}[b]	$10^4 k_1$ s^{-1}[c]
2-methyl-1,3-dioxolane	469.8	1	15.83 ± 4.60	3.96 ± 0.07
		6.22	35.40 ± 6.34	3.90 ± 0.09
2,2-dimethyl-1,3-dioxolane	480.3	1	12.89 ± 3.80	3.74 ± 0.07
		6.22	37.11 ± 5.66	3.81 ± 0.12
cyclopentanone ethylene ketal	470.1	1	8.95 ± 2.53	5.82 ± 0.14
		6.22	32.23 ± 4.41	5.71 ± 0.10

[a] S, surface area; V, volume. [b] A clean Pyrex vessel was used. [c] The vessel was deactivated with allyl bromide.

The thermal decomposition experiments were carried out in the presence of the free radical suppressor propene in order to prevent any possible chain reactions. The effect of different proportions of propene in this process is shown in Table 2. No induction period was observed. The rate coefficient was reproducible with a relative deviation of less than 5% at a given temperature.

The stoichiometries of reactions 4−6, up to a 75% reaction, were verified by comparing the extent of decomposition of the substrates from pressure measurements to that obtained from quantitative gas liquid chromatographic (GLC) analyses of the starting material and/or the corresponding products' formation (Table 3).

The rates of decomposition were found to be invariable with changes in the initial pressure of the substrates (Table 4), and the first-order plots are satisfactorily linear, up to 75% decomposition of the reactants. The temperature dependence of the reaction in the deactivated vessel with the product of decomposition of allyl bromide and in the presence of the free radical inhibitor propene together, with the corresponding Arrhenius equation, are given in Table 5. The errors were estimated to 90% confidence limits from a least-squares procedure.

Table 2. Effect of the Free Radical Chain Inhibitor on Rates

substrate	temp (°C)	P_s[a] (Torr)	P_i[b] (Torr)	P_i/P_s	$10^4 k_1$ (s^{-1})
2-methyl-1,3-dioxolane	469.8	49	–	–	6.64
		63	70	1.1	5.33
		54	81	1.5	3.96
		52	100	1.9	3.78
		66	158	2.4	3.90
2,2-dimethyl-1,3-dioxolane	480.3	54	–	–	1.59
		41	37	0.9	3.36
		64	90	1.4	3.78
		56	123	2.2	3.56
		68	224	3.3	3.62
cyclopentanone ethylene ketal	470.1	56	–	–	3.27
		46	93	1.0	5.04
		58	140	2.4	5.86
		44	170	3.4	5.70
		62	285	4.6	5.96

[a] P_s, pressure of substrate. [b] P_i, pressure of free radical inhibitor propene.

The values of log A from 13.61 to 14.16, listed in Table 6, are reasonable values for a four-membered cyclic transition state type of mechanism, as suggested by Benson.[17] According to product formations and the kinetic and thermodynamic parameters, the mechanisms of these reactions may be considered to proceed via a concerted four-membered cyclic transition state in the rate-determining step, as described in reactions 7−9.

The proposed mechanism for product formation from 2-methyl-1,3-dioxolane is shown below.

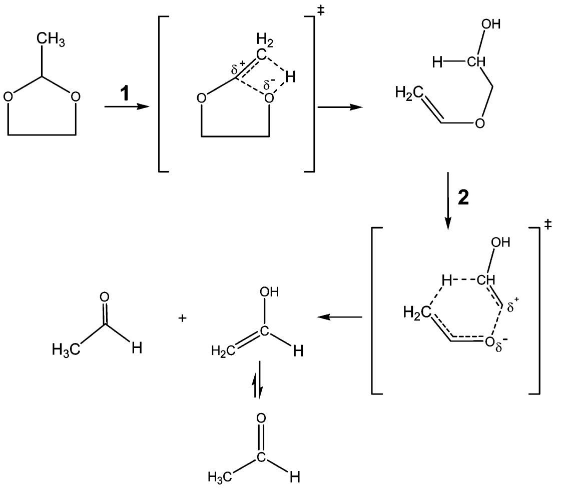

(7)

As described above for the decomposition of 2,2-diethoxypropane,[10] the intermediate formed in 2-methyl-1,3-dioxolane undergoes further decomposition at the high-temperature condition. This type of reaction has been reported for alkyl vinyl ethers.[11,12] The proposed mechanism proceeds through a six-centered cyclic transition state as shown in step 2 (reaction 7). Similar decomposition occurs with the intermediates of 2,2-dimethyl-1,3-dioxolane and cyclopentanone ethylene ketal shown below.

Table 3. Stoichiometry of the Reaction[a]

substrate	temp (°C)	parameters	value					
2-methyl-1,3-dioxolane[b]	469.8	time (min)	5	10	15	20	40	60
		reaction (%) (pressure)	10.3	18.5	28.4	35.4	58.3	72.9
		substrate (%) (GLC)	11.0	19.4	28.1	35.3	59.3	72.5
2,2-dimethyl-1,3-dioxolane[b]	480.3	time (min)	5	10	15	20	40	60
		reaction (%) (pressure)	10.1	20.1	28.8	35.9	60.6	76.1
		substrate (%) (GLC)	8.8	19.5	28.0	35.3	59.5	75.4
		acetone (%) (GLC)	9.7	20.3	28.8	36.0	60.4	75.2
cyclopentanone ethylene ketal[b]	470.1	time (min)	2.5	5	10	15	20	40
		reaction (%) (pressure)	8.3	17.4	29.3	40.7	50.4	76.2
		substrate (%) (GLC)	8.0	16.2	29.0	39.9	48.3	75.5
		cyclopentanone (%) (GLC)	8.4	16.4	29.7	40.1	48.4	75.0

[a]Reaction vessels were seasoned with allyl bromide. [b]Values determined in the presence of the propene inhibitor.

Table 4. Invariability of the Rate Coefficients from the Initial Pressure[a]

substrate	temp (°C)	parameters	value				
2-methyl-1,3-dioxolane	469.8	P_0 (Torr)	46	57	69	86.5	113
		$10^4 k_1$ (s^{-1})	4.09	4.01	3.90	3.94	3.96
2,2-dimethyl-1,3-dioxolane	480.3	P_0 (Torr)	51	53	67	72	85
		$10^4 k_1$ (s^{-1})	3.71	3.95	3.51	3.78	3.77
cyclopentanone ethylene ketal	470.1	P_0 (Torr)	55	52	69.5	86	88
		$10^4 k_1$ (s^{-1})	5.75	5.86	5.83	5.96	5.71

[a]The results are from the GLC analyses.

Table 5. Variation of the Rate Coefficients with Temperature[a]

2-Methyl-1,3-dioxolane					
temperature (°C)	459.7	465.1	469.8	475.0	479.7
$10^4 k_1$ (s^{-1})	2.26	3.00	3.84	5.05	6.50
$\log k_1 = (13.61 \pm 0.12) - (242.1 \pm 1.0)$ kJ mol^{-1} $(2.303RT)^{-1}$; $r = 0.9997$					
2,2-Dimethyl-1,3-dioxolane					
temperature (°C)	470.2	475.1	480.3	485.0	490.0
$10^4 k_1$ (s^{-1})	2.17	2.83	3.71	4.86	6.40
$\log k_1 = (14.16 \pm 0.14) - (253.7 \pm 2.0)$ kJ mol^{-1} $(2.303RT)^{-1}$; $r = 0.9998$					
Cyclopentanone Ethylene Ketal					
temperature (°C)	460.0	465.6	470.1	475.3	480.4
$10^4 k_1$ (s^{-1})	3.40	4.50	5.84	7.60	9.80
$\log k_1 = (13.48 \pm 0.11) - (238.0 \pm 1.6)$ kJ mol^{-1} $(2.303RT)^{-1}$; $r = 0.9998$					

[a]Obtained by GLC analysis.

The proposed mechanism for product formation from 2,2-dimethyl-1,3-dioxolane is shown below.

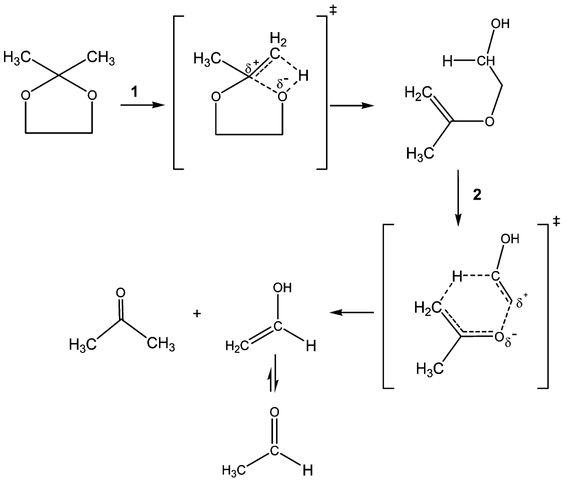

(8)

The mechanism suggested for product formation from cyclopentanone ethylene ketal is as follows:

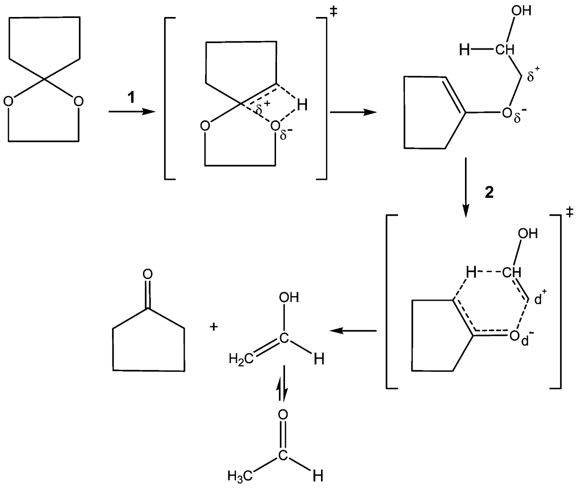

(9)

In order to support or modify the proposed mechanisms described in reactions 7–9, a theoretical study of these decomposition reactions in the present work was additionally carried out.

IV. COMPUTATIONAL METHODS AND MODEL

The electronic structure calculations were performed using density functional theory (DFT) methods: Becke's three-parameter formulation from functional Lee, Yang, and Parr [B3LYP/6-31G(d,p) and B3LYP/6-31++G(d,p)],[18−20] and Perdew–Wang 1991 correlation functional [MPW1PW9/6-31G(d,p) and MPW1PW91/6-31++G(d,p)].[21] The calculations have been performed with Gaussian 03.[22] Default parameters were used for convergence (e.g., Berny analytical gradient optimization routine, convergence on the density matrix, 10^{-9} atomic unit; threshold value for maximum

Table 6. Kinetic and Thermodynamic Parameters at 480.0°C

substrate	10^4k_1 (s^{-1})	E_a (kJ/mol)	log A (s^{-1})	$\Delta S^{\ddagger}$ (J mol^{-1} K^{-1})	$\Delta H^{\ddagger}$ (kJ/mol)	$\Delta G^{\ddagger}$ (kJ/mol)
2-methyl-1,3-dioxolane	6.46	242.1 ± 1.0	13.61 ± 0.12	−0.43	235.8	236.1
2,2-dimethyl-1,3-dioxolane	3.63	253.7 ± 2.0	14.16 ± 0.14	10.10	247.4	239.8
cyclopentanone ethylene ketal	9.32	238.0 ± 1.6	13.48 ± 0.11	−2.92	231.7	233.9

displacement, 0.0018 Å; and maximum force, 0.00045 hartree/bohr. Location of transition state (TS) structures was performed using the Quadratic Synchronous Transit (QST) protocol. All structures were fully optimized, and frequency calculations were performed to ensure the absence of any imaginary frequencies on local minima and the presence of a single imaginary frequency on TSs. Intrinsic reaction coordinate (IRC) calculations were carried out to confirm the reaction pathways (Supporting Information).

Thermodynamic parameters were calculated from frequency calculations {i.e., zero-point vibrational energy (ZPVE), temperature corrections [$E(T)$], and absolute entropies [$S(T)$]}, assuming ideal gas behavior from the harmonic frequencies and moments of inertia by standard methods.[23] Frequency values, moments of inertia, and thermochemistry results are included as Supporting Information. We used average temperature and pressure within the experimental range. Scaling factors for frequencies and zero-point energies were taken from the literature[24,25] (Table 7)

Table 7. Scaling Factors for Frequency Calculations at 753.15 K (480 °C)

method	T (K)	P (atm)	scaling factors
	2-Methyl-1,3-dioxolane		
B3LYP/6-31++G(d,p)	753.15	0.11	0.964
	2,2-Dimethyl-1,3-dioxolane		
MPW1PW91/6-31G(d,p)	753.15	0.11	0.952
	Cyclopentanone Ethylene Ketal		
MPW1PW91/6-31G(d,p)	753.15	0.11	0.952

The rate constants were obtained using the canonical TST. The experimental enthalpy, entropy, and free energy of activation are obtained from the energy of activation and log A using the Arrhenius and Eyring equations.[26] Theoretical energies of activation, log A, and rate coefficients are derived from the enthalpy and entropy of activation obtained in the frequency calculations. Detailed description and equations are described in previous works.[27,28]

Theoretical Results. *Kinetic and Thermodynamic Parameters.* Calculated activation parameters for the rate-determining step of the thermal decomposition of 2-methyl-1,3-dioxolane, 2,2-dimethyl-1,3-dioxolane, and cyclopentanone ethylene ketal are presented in Table 8. The second step in all cases has a lower energy of activation, thereby confirming that the first step is rate-determining, derived from the B3LYP/6-31++G(d,p) and MPW1PW91/6-31G(d,p) level of theory, as shown in Figures 1−3.

Comparing calculated parameters to the experimental values, we obtain good agreement for energies of activation and, consequently, for enthalpies of activation at B3LYP/6-31++G(d,p) for the decomposition reaction of 2-methyl-1,3-dioxolane. Conversely, for 2,2-dimethyl-1,3-dioxolane and cyclopentanone ethylene ketal, B3LYP/6-31++G(d,p) underestimates the enthalpy and energies of activation. The calculated values were closer to the experimental values with the MPW1PW91/6-31G(d,p) method. In all cases, the calculated entropy of activation was more negative than the experimental value. The divergences observed are possibly due to the use of the harmonic approximation and the existence of low-frequency modes. These vibrational modes are highly unharmonic and may contribute significantly to the entropy. Anharmonic frequency calculations, hindered-rotor and free-rotor models, have been used for this purpose; however, we have found that enthalpies of activation and consequently energies of activation can be used to explain the preferred reaction path.

To further study the nature of these reactions and the TS involved in the processes, we studied the geometrical parameters, NBO charges, and bond orders as described in the following sections.

For the analysis of geometrical parameters, NBO charges, and bond orders, we have selected the B3LYP/6-31++G(d,p) method for 2-methyl-1,3-dioxolane and the MPW1PW91/6-31G(d,p) method for 2,2-dimethyl-1,3-dioxolane and cyclopentanone ethylene ketal.

Transition State and Mechanism. The quadratic synchronous transit method allowed us to locate the transition state structures of the above reactions. The optimized structures for reactants, the TS, and products of the thermal decomposition of 2-methyl-1,3-dixolane, 2,2-1,3-dimethyldioxolane, and cyclopentanone ethylene ketal are displayed in Figures 4−6.

The structures of the transition states are four-centered geometries comprising atoms C_1, C_2, O_3, and H_4. Structural parameters of reactant, TS, and product of these reactions are reported in Tables 9−11; atom numbers are shown in Schemes 3−5.

In the thermal decomposition of 2-methyl-1,3-dioxolane, 2,2-dimethyl-1,3-dioxolane, and cyclopentanone ethylene ketal, the most significant geometrical change is the elongation of the $C_2{-}O_3$ bond from 1.43 to 2.39 Å in the TS for 2-methyl-1,3-dioxolane and from 1.42 to 2.25 Å in the TS for both 2,2-dimethyl-1,3-dioxolane and cyclopentanone ethylene ketal. The elongation of the $H_4{-}C_1$ bond is also important as this distance changes from 1.09 to 1.24 Å in the TS for 2-methyl-1,3-dioxolane and cyclopentanone ethylene ketal; this change is greater for 2,2-dimethyl-1,3-dioxolane (from 1.09 to 1.28 Å). The $C_1{-}C_2$ distance shortens from 1.51−1.54 to 1.43−1.44 Å reflecting the change from a single to a double bond. For all substrates, the four atoms involved in the TS lie in a plane, as seen in the dihedrals.

NBO Charges. The changes in electronic structure along the reaction pathway may be followed by NBO charges. The NBO charges of atoms involved in the reaction changes in the reactant, TS, and products of the compounds in this study are reported in Tables 12−14. Atom numbers are shown in Schemes 3−5.

For the three substrates, there is an increase in electron density at O_3 of an ∼0.18 negative charge increase for 2-methyl-1,3-dioxolane and 2,2-dimethyl-1,3-dioxolane, and a 0.2 negative charge increase for cyclopentanone ethylene ketal. At C_2 the changes are very small in the TS for the three substrates. There is

Table 8. Calculated Kinetic and Thermodynamic Parameters of Activation at 480.0 °C

method	E_a (kJ/mol)	log A	$\Delta S^{\ddagger}$ (J mol^{-1} K^{-1})	$\Delta H^{\ddagger}$ (kJ/mol)	$\Delta G^{\ddagger}$ (kJ/mol)
2-Methyl-1,3-dioxolane					
experimental	242.1	13.61	−0.43	235.8	236.1
B3LYP/6-31G(d,p)	253.7	12.83	−15.23	247.5	259.0
B3LYP/6-31++G(d,p)	247.1	12.82	−15.52	240.8	252.5
MPW1PW91/6-31G(d,p)	269.2	12.86	−14.81	263.8	274.1
MPW1PW91/6-31++G(d,p)	265.2	12.78	−16.23	258.9	271.1
Fast step (B3LYP/6-31++G(d,p))	172.3	11.82	−34.61	166.1	192.13
2,2-Dimethyl-1,3-dioxolane					
experimental	253.7	14.16	10.10	247.4	239.8
B3LYP/6-31G(d,p)	235.1	13.29	−6.56	228.8	233.75
B3LYP/6-31++G(d,p)	225.0	13.42	−3.98	218.8	221.76
MPW1PW91/6-31G(d,p)	246.2	13.17	−8.72	239.9	246.47
MPW1PW91/6-31++G(d,p)	239.3	13.33	−5.65	233.1	237.33
fast step (MPW1PW91/6-31G(d,p))	163.1	12.57	−20.23	156.8	172.05
Cyclopentanone Ethylene Ketal					
experimental	238.0	13.48	−2.92	232.4	233.9
B3LYP/6-31G(d,p)	229.6	12.92	−13.57	223.3	233.52
B3LYP/6-31G++(d,p)	217.8	12.73	−17.27	211.6	224.57
MPW1PW91/6-31G(d,p)	242.2	12.91	−13.81	236.0	246.36
MPW1PW91/6-31++G(d,p)	233.6	12.94	−13.23	227.3	237.30
fast step (MPW1PW91/6-31G(d,p))	162.7	12.02	−30.89	156.4	179.66

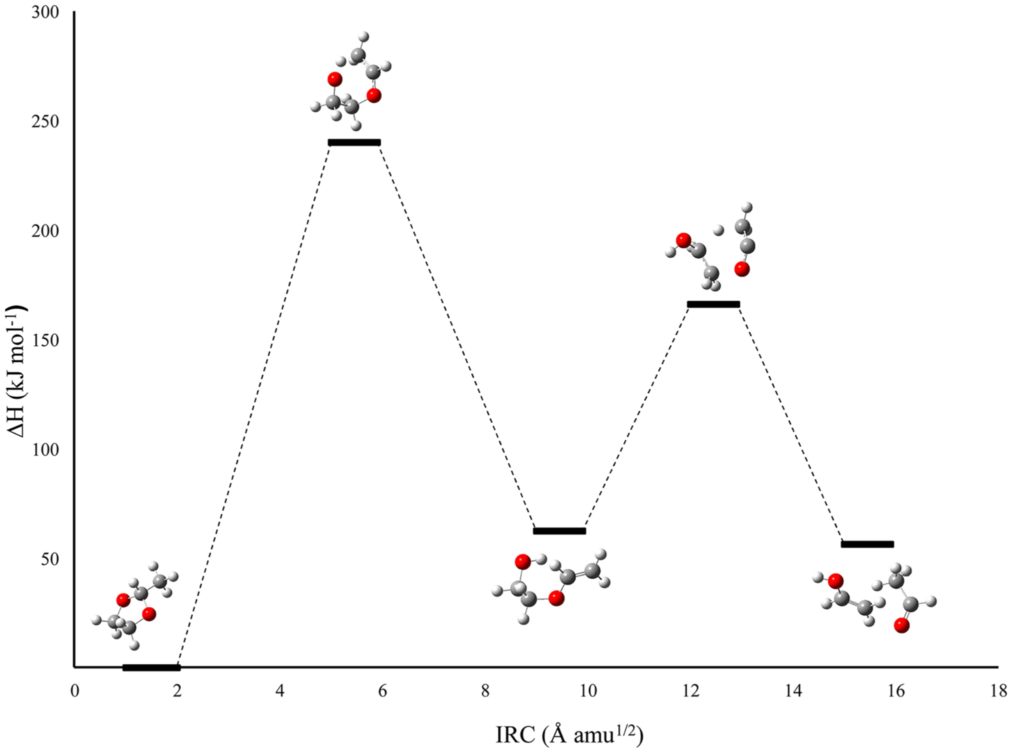

Figure 1. Reaction profile for the thermal decomposition of 2-methyl-1,3-dioxolane at the B3LYP/6-31++G(d,p) level of theory.

a similar increase in positive charge at H_4 in the TS by 0.15, 0.16, and 0.15 for 2-methyl-1,3-dioxolane, 2,2-dimethyl-1,3-dioxolane, and cyclopentanone ethylene ketal, respectively, as C_1 becomes more electron-rich, increasing the negative charge by 0.15, 0.10, and 0.13 for 2-methyl-1,3-dioxolane, 2,2-dimethyl-1,3-dioxolane, and cyclopentanone ethylene ketal, respectively. These changes reflect the C_1−H_4 and C_2−O_3 bond breaking in the TS, described in the proposed mechanism.

Bond Order Analysis. NBO calculations were used to calculate bond orders aimed at describing the progress along different reaction coordinates.[29−31] Wiberg bond indexes[32] were calculated using the Natural Bond Orbital (NBO) program[33] with Gaussian 03. The reaction mechanism involving bond breaking and making may be identified by the synchronicity (Sy) concept proposed by Moyano et al.[34] as described in the following equations:

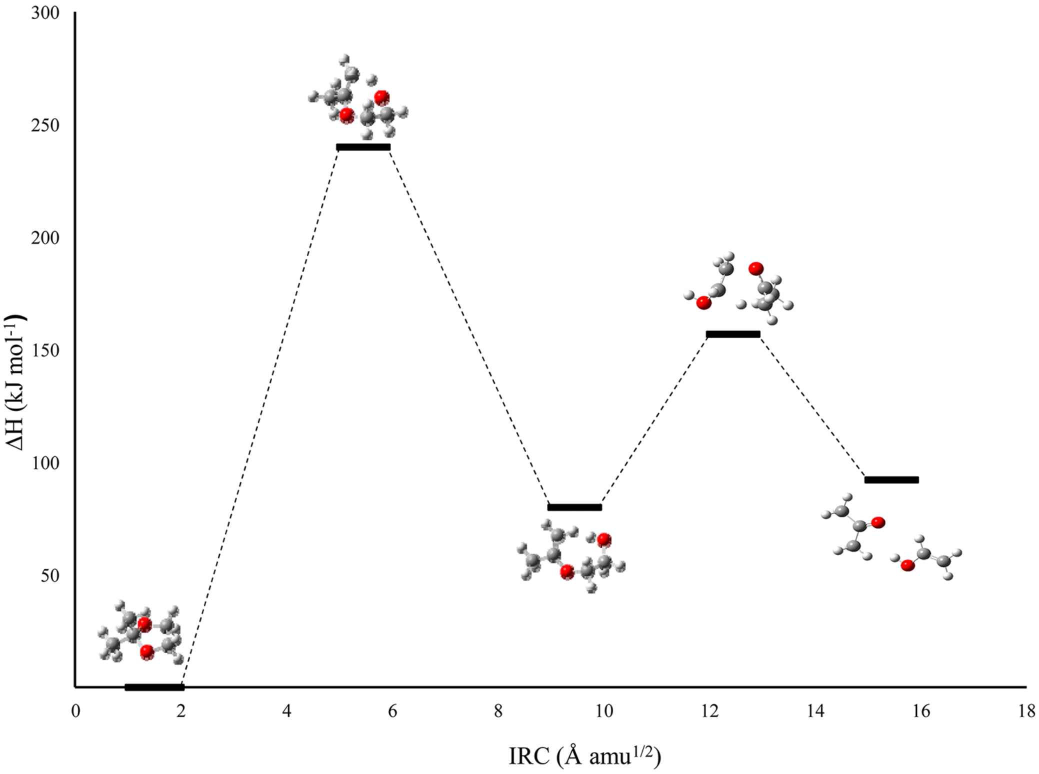

Figure 2. Reaction profile for the thermal decomposition of 2,2-dimethyl-1,3-dioxolane at the MPW1PW91/6-31G(d,p) level of theory.

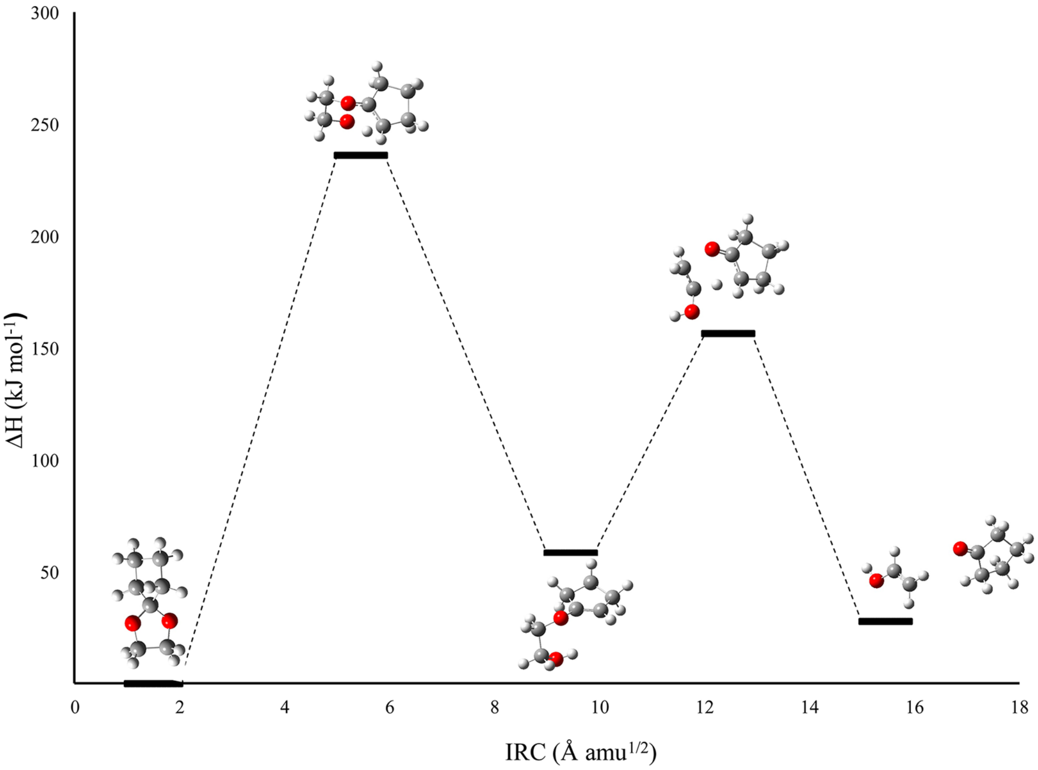

Figure 3. Reaction profile for the thermal decomposition of cyclopentanone ethylene ketal at the MPW1PW91/6-31G(d,p) level of theory.

$$Sy = 1 - \left[\sum_{i=1}^{n} |\delta B_i - \delta B_{av}|/\delta B_{av}\right] \Big/ 2n - 2$$

The synchronicity parameter in concerted reactions varies from 0 to 1; the value 1 represents a synchronic concerted process in which all bonds are formed and broken in the same way in the TS.

δB_i indicates change in i bond order, and n is the number of bonds directly involved in the reaction. The relative variation of the bond index is obtained from

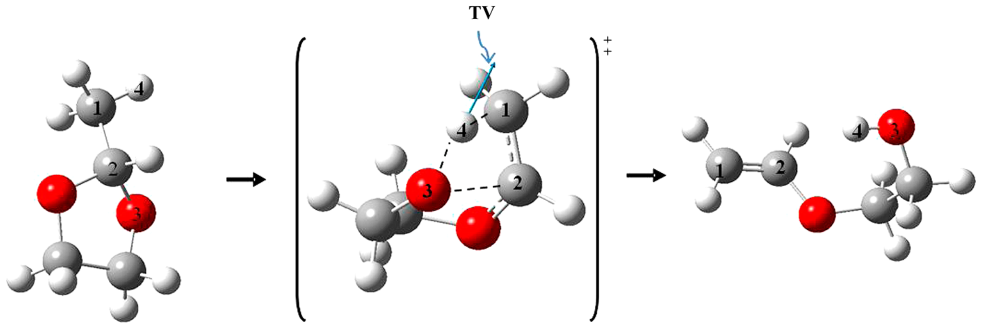

Figure 4. Structures of reactant (left), transition state (TS) (center), and products (right) of the gas-phase decomposition of 2-methyl-1,3-dioxolane, optimized at the B3LYP/6-31++G(d,p) level of theory.

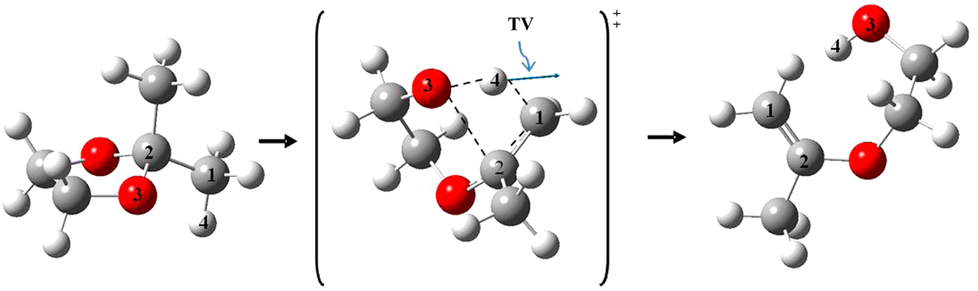

Figure 5. Structures of reactant (left), transition state (TS) (center), and products (right) of the gas-phase decomposition of 2,2-dimethyl-1,3-dioxolane, optimized at the MPW1PW91/6-31G(d,p) level of theory.

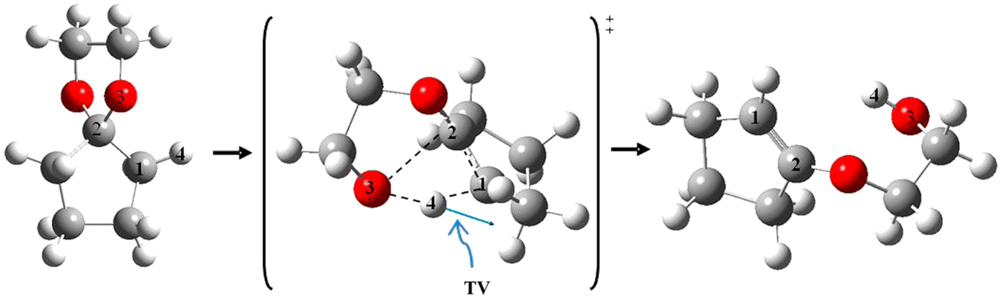

Figure 6. Structures of reactant (left), transition state (TS) (center), and products (right) of the gas-phase decomposition of cyclopentanone ethylene ketal, optimized at the MPW1PW91/6-31G(d,p) level of theory.

Table 9. Structural Parameters for the Optimized Reactant (R), Transition State (TS), and Products (P) from the 2-Methyl-1,3-dioxolane Decomposition with the B3LYP/6-31++G(d,p) Method

	Atomic distances (Å)			
	C_1-C_2	C_2-O_3	O_3-H_4	H_4-C_1
R	1.510	1.429	2.680	1.093
TS	1.433	2.391	1.463	1.239
P	1.336	3.171	0.967	3.318
	Dihedral (deg)			
	$C_1-C_2-O_3-H_4$	$C_2-O_3-H_4-C_1$	$O_3-H_4-C_1-C_2$	$H_4-C_1-C_2-O_3$
TS	−2.522	4.369	−5.771	2.356
	Imaginary Frequency (cm^{-1})			
	TS		1459.7	

Table 10. Structural Parameters for the Optimized Reactant (R), Transition State (TS), and Products (P) from the 2,2-Dimethyl-1,3-dioxolane Decomposition with the MPW1PW91/6-31G(d,p) Method

	Atomic Distance (Å)			
	C_1-C_2	C_2-O_3	O_3-H_4	H_4-C_1
R	1.523	1.417	2.704	1.092
TS	1.432	2.248	1.381	1.275
P	1.339	3.345	0.963	2.523
	Dihedral (deg)			
	$C_1-C_2-O_3-H_4$	$C_2-O_3-H_4-C_1$	$O_3-H_4-C_1-C_2$	$H_4-C_1-C_2-O_3$
TS	−1.504	2.518	−3.238	1.334
	Imaginary Frequency (cm^{-1})			
	TS		1653.2	

$$\delta B_i = [B_i^{\mathrm{TS}} - B_i^{\mathrm{R}}]/[B_i^{\mathrm{P}} - B_i^{\mathrm{R}}]$$

The superscripts R, TS, and P indicate reactant, transition state, and product, respectively.

Bond orders were estimated using Wiberg bond indexes B_i, calculated for the bonds involved in the reaction changes (i.e., C_1-C_2, C_2-O_3, O_3-H_4, and H_4-C_1; Tables 15−17).

Table 11. Structural Parameters for the Optimized Reactant (R), Transition State (TS), and Products (P) from the Cyclopentanone Ethylene Ketal Decomposition with the MPW1PW91/6-31G (d,p) Method

	Atomic Distance (Å)			
	C_1-C_2	C_2-O_3	O_3-H_4	H_4-C_1
R	1.539	1.418	2.482	1.092
TS	1.441	2.365	1.443	1.237
P	1.336	4.704	0.960	6.613
	Dihedral (deg)			
	$C_1-C_2-O_3-H_4$	$C_2-O_3-H_4-C_1$	$O_3-H_4-C_1-C_2$	$H_4-C_1-C_2-O_3$
TS	0.827	−1.475	1.920	−0.765
	Imaginary Frequency (cm^{-1})			
TS	1445.85			

Scheme 3

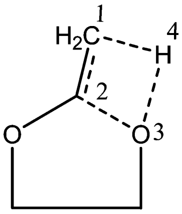

Scheme 4

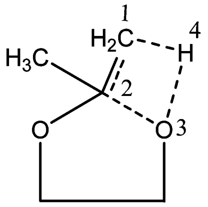

Scheme 5

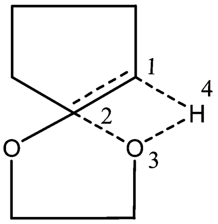

Table 12. NBO Charges of the Atoms Involved in the 2-Methyl-1,3-dioxolane Thermal Decomposition from the B3LYP/6-31++G(d,p) Calculations

	R	TS	P
C_1	−0.69	−0.84	−0.54
C_2	0.39	0.41	0.11
O_3	−0.61	−0.79	−0.77
H_4	0.24	0.39	0.50

Table 13. NBO Charges of the Atoms Involved in the 2,2-Dimethyl-1,3-dioxolane Thermal Decomposition from the MPW1PW91/6-31G(d,p) Calculations

	R	TS	P
C_1	−0.76	−0.86	−0.77
C_2	0.59	0.58	0.31
O_3	−0.59	−0.77	−0.76
H_4	0.25	0.41	0.27

Table 14. NBO Charges of the Atoms Involved in the Cyclopentanone Ethylene Ketal Thermal Decomposition from the MPW1PW91/6-31G(d,p) Calculations

	R	TS	P
C_1	−0.53	−0.66	−0.31
C_2	0.59	0.61	0.32
O_3	−0.59	−0.79	−0.77
H_4	0.26	0.41	0.49

Table 15. Wiberg Bond Index of the Reactant (R), Transition State (TS), and Products (P) for the 2-Methyl-1,3-dioxolane Thermal Decomposition from the B3LYP/6-31++G(d,p) Calculation

	C_1-C_2	C_2-O_3	O_3-H_4	H_4-C_1	Sy	δB_{av}
B_i^R	1.02	0.90	0.00	0.92	0.75	0.41
B_i^{TS}	1.23	0.25	0.22	0.57		
B_i^P	1.90	0.01	0.74	0.00		
$\%E_v$	24.31	72.23	30.09	38.67		

Table 16. Wiberg Bond Index of the Reactant (R), Transition State (TS), and Products (P) for the 2,2-Dimethyl-1,3-dioxolane Thermal Decomposition from the MPW1PW91/6-31G(d,p) Calculation

	C_1-C_2	C_2-O_3	O_3-H_4	H_4-C_1	Sy	δB_{av}
B_i^R	0.99	0.89	0.00	0.92	0.80	0.44
B_i^{TS}	1.23	0.27	0.26	0.51		
B_i^P	1.87	0.00	0.74	0.00		
$\%E_v$	26.81	70.19	34.81	44.74		

Table 17. Wiberg Bond Index of the Reactant (R), Transition State (TS), and Products (P) for the Cyclopentanone Ethylene Ketal Thermal Decomposition from the MPW1PW91/6-31G(d,p) Calculation

	C_1-C_2	C_2-O_3	O_3-H_4	H_4-C_1	Sy	δB_{av}
B_i^R	0.98	0.90	0.00	0.90	0.75	0.43
B_i^{TS}	1.19	0.22	0.23	0.53		
B_i^P	1.81	0.00	0.75	0.00		
$\%E_v$	25.30	75.56	30.67	41.11		

Bond order indexes describing the bond formation and breaking in the thermal decomposition reactions of 2-methyl-1,3-dioxolane, 2,2-dimethyl-dioxolane, and cyclopentanone ethylene ketal are shown in Tables 15−17. In comparison with the other bonds in the TS, the breaking of the C_2-O_3 bond is more complete at 72%, 70%, and 76% for 2-methyl-1,3-dioxolane, 2,2-dimethyl-dioxolane, and cyclopentanone ethylene ketal, repectively.

V. CONCLUSIONS

In the present joint experimental and theoretical work, we have studied the thermal decomposition reactions in the gas phase of a series of dioxolanes (i.e., 2-methyl-1,3-dioxolane, 2,2-dimethyl-1,3-dioxolane, and cyclopentanone ethylene ketal) and aimed to propose a reasonable mechanism in accordance with product formation and experimental and calculated kinetic and thermodynamic parameters.

These reactions in the presence of the free radical inhibitor propene are homogeneous and unimolecular, and they follow first-order law kinetics. The dioxolanes in this study decompose through a concerted four-centered cyclic TS mechanism, in the rate-determining step, to produce an alkyl vinyl ether intermediate product. The intermediate alkyl vinyl ether further decomposes in a fast step through a six-centered TS. For 2-methyl-1,3-dioxolane, the final product is acetaldehyde; for 2,2-dimethyl-1,3-dioxolane, the final products are acetone and acetaldehyde, and for cyclopentanone ethylene ketal, the final products are cyclopentanone and acetaldehyde.

The mechanism was studied by DFT calculations. Calculated enthalpies and, consequently, energies of activation are in agreement with experimental values, supporting the proposed mechanism. The experimental activation energies are similar for 2-methyl-1,3-dioxolane and cyclopentanone ethylene ketal, and about 10 kJ higher for 2,2-dimethyl-1,3-dioxolane. The electron density at the central carbon in the dioxolane moiety does not change from the reactant to the TS for the three substrates. The introduction of a second methyl substituent in 2,2-dimethyl-1,3-dioxolane produces a moderate increase in E_a and also in ΔS. In cyclopentanone ethylene ketal, it is not observed despite the similar substitution at the central dioxolane carbon. It appears that the substitution and strain effects cancel each other out, and consequently, the E_a and ΔH of cyclopentanone ethylene ketal and 2-methyl-1,3-dioxolane are similar.

The breaking of the C−O bond is the most advanced reaction coordinate in the TS, more so for cyclopentanone ethylene ketal involving the breaking of the spiro structure. These reactions appear to proceed as concerted nonsynchronous processes, governed by the breaking of the C−O bond in the rate-determining step.

■ ASSOCIATED CONTENT

Ⓢ Supporting Information

IRC obtained from gas-phase thermal decomposition kinetics of 2-methyl-1,3-dioxolane, 2,2-dimethyl-1,3-dioxolane, and cyclopentanone ethylene ketal. This material is available free of charge via the Internet at http://pubs.acs.org.

■ AUTHOR INFORMATION

Corresponding Author

*E-mail: chuchani@ivic.gob.ve.

Notes

The authors declare no competing financial interest.

■ REFERENCES

(1) Molera, M.; Centeno, J.; Orza, J. *J. Chem. Soc.* **1963**, 2234−2241.

(2) Molera, M.; Fernandez-Biarge, J.; Centeno, J.; Arévalo, L. *J. Chem. Soc.* **1963**, 2311−2320.

(3) Molera, M.; Dominguez, G. *An. R. Soc. Esp. Fis. Quim.* **1963**, *11*, 639−648.

(4) Molera, M.; Pereira, G. *An. Fis. Quim.* **1966**, *62*, 661−666.

(5) Molera, M.; Pereira, G. *An. Fis. Quim.* **1966**, *62*, 667−675.

(6) Garcia Dominguez, J. A.; Molera, M. J. *An. Fis. Quim.* **1970**, *70*, 186−188.

(7) Mora, J. R.; Dominguez, R. M.; Herize, A.; Tosta, M.; Chuchani, G. *J. Phys. Org. Chem.* **2008**, *21*, 359−364.

(8) Mora, J. R.; Maldonado, A.; Domínguez, R. M.; Chuchani, G. *J. Phys. Org. Chem.* **2010**, *23*, 845−852.

(9) Rosas, F.; Domínguez, R. M.; Tosta, M.; Mora, J. R.; Márquez, E.; Córdova, T.; Chuchani, G. *J. Phys. Org. Chem.* **2010**, *23*, 743−750.

(10) Rosas, F.; Maldonado, J.; Lezama, J.; Domínguez, R. M.; Mora, J. R.; Córdova, T.; Chuchani, G. *J. Phys. Chem. A* **2012**, *116*, 846−854.

(11) Smith, G. G.; Kelly, F. W. *Prog. React. Kinet.* **1971**, *8*, 75−234.

(12) Awan, I. A.; Flowers, M. C. *J. Chem. Soc. Pak.* **1988**, *10* (3), 363−368.

(13) Maccoll, A. *J. Chem. Soc.* **1955**, 965−973.

(14) Swinbourne, E. S. *Aust. J. Chem.* **1958**, *11*, 314−330.

(15) Dominguez, R. M.; Herize, A.; Rotinov, A.; Alvarez-Aular, A.; Visbal, G.; Chuchani, G. *J. Phys. Org. Chem.* **2004**, *17*, 399−408.

(16) Espitia, L.; Meneses, R.; Domínguez, R. M.; Tosta, M.; Herize, A.; Lafont, J.; Chuchani, G. *Int. J. Chem. Kinet.* **2009**, *41*, 145−152.

(17) O'Neal, H. E.; Benson, S. W. *J. Phys. Chem.* **1967**, *71*, 2903−2921.

(18) Becke, A. D. *Phys. Rev. A* **1988**, *34*, 3098−3100.

(19) Becke, A. D. *J. Chem. Phys.* **1993**, *98*, 1372−1377.

(20) Becke, A. D. *J. Chem. Phys.* **1993**, *98*, 5648−5652.

(21) Perdew, J. P.; Wang, Y. *Phys. Rev. B* **1992**, *45*, 13244−13249.

(22) Frisch, M. J.; Trucks, G. W.; Schlegel, H. B.; Scuseria, G. E.; Robb, M. A.; Cheeseman, J. R.; Montgomery, J. A., Jr.; Vreven, T.; Kudin, K. N.; Burant, J. C.; et al. *Gaussian 03*, revision C.02; Gaussian, Inc.: Wallingford, CT, 2004.

(23) McQuarrie, D. *Statistical Mechanics*; Harper & Row: New York, 1986.

(24) Foresman, J. B.; Frish, Æ. *Exploring Chemistry with Electronic Methods*, 2nd ed.; Gaussian, Inc.: Pittsburgh, PA, 1996.

(25) (a) Scale factors in http://cccbdb.nist.gov/vibscalejust.asp. (b) Database of Frequency Scaling Factors for Electronic Structure Methods. http://comp.chem.umn.edu/truhlar/freq_scale.htm.

(26) Benson, S. W. *The Foundations of Chemical Kinetics*; McGraw-Hill: New York, 1960.

(27) Cordova, T.; Rotinov, A.; Chuchani, G. *J. Phys. Org. Chem.* **2004**, *17*, 148−151.

(28) Marquez, E.; Dominguez, R. M.; Mora, J. R.; Cordova, T.; Chuchani, G. *J. Phys. Chem. A* **2010**, *114* (12), 4203−4209.

(29) Lendvay, G. *J. Phys. Chem.* **1989**, *93*, 4422−4429.

(30) Reed, A. E.; Weinstock, R. B.; Weinhold, F. *J. Chem. Phys.* **1985**, *83* (2), 735−746.

(31) Reed, A. E.; Curtiss, L. A.; Weinhold, F. *Chem. Rev.* **1988**, *88*, 899−926.

(32) Wiberg, K. B. *Tetrahedron* **1968**, *24*, 1083−1096.

(33) Reed, A. E.; Carpenter, J. E.; Weinhold, F. NBO version 3.1. *J. Chem. Phys.* **1985**, *83*, 735−746.

(34) Moyano, A.; Pericá, M. A.; Valenti, E. *J. Org. Chem.* **1989**, *54*, 573−582.